MULTISCALE MODEL. SIMUL.
Vol. 6, No. 1, pp. 135–157

CONCURRENT MULTISCALE COMPUTING OF DEFORMATION MICROSTRUCTURE BY RELAXATION AND LOCAL ENRICHMENT WITH APPLICATION TO SINGLE-CRYSTAL PLASTICITY*

SERGIO CONTI†, PATRICE HAURET‡, AND MICHAEL ORTIZ‡

Abstract. This paper is concerned with the effective modeling of deformation microstructures within a *concurrent multiscale computing* framework. We present a rigorous formulation of concurrent multiscale computing based on relaxation; we establish the connection between concurrent multiscale computing and enhanced-strain elements; and we illustrate the approach in an important area of application, namely, single-crystal plasticity, for which the explicit relaxation of the problem is derived analytically. This example demonstrates the vast effect of microstructure formation on the macroscopic behavior of the sample, e.g., on the force/travel curve of a rigid indentor. Thus, whereas the unrelaxed model results in an overly stiff response, the relaxed model exhibits a proper limit load, as expected. Our numerical examples additionally illustrate that ad hoc element enhancements, e.g., based on polynomial, trigonometric, or similar representations, are unlikely to result in any significant relaxation in general.

Key words. multiscale computing, relaxation, microstructure, finite elements, enhanced strain, single-crystal plasticity

AMS subject classifications. 74G65, 74C05

DOI. 10.1137/060662332

1. Introduction.

The problem addressed in this paper concerns the effective modeling of deformation microstructures within a *concurrent multiscale computing* framework. In many applications of interest, materials develop fine microstructure on multiple length and time scales in response to loading [5, 53, 58, 49]. Examples of such microstructures include martensite; subgrain dislocation structures; dislocation walls and networks; ferroelectric domains; shear bands; spall planes; and others. In addition, materials such as polycrystalline metals may exhibit processing microstructure from the outset, prior to the onset of deformation. The macroscopic behavior of such materials is too complex to be amenable to modeling based on simple representational schemes, such as afforded by continuum thermodynamics, symmetry groups, linearization, polynomial approximations, empirical fitting and calibration, and other similar schemes. Indeed, empirical models are a major source of error and uncertainty in engineering applications, and the empirical paradigm does not offer a systematic means of reducing such error and uncertainty.

Multiscale modeling aims to eliminate empiricism and uncertainty from material models by systematically identifying the rate-controlling mechanisms at all scales and the fundamental laws that govern those mechanisms, and by bridging the relevant

*Received by the editors June 7, 2006; accepted for publication (in revised form) October 5, 2006; published electronically March 22, 2007.
http://www.siam.org/journals/mms/6-1/66233.html

†Fachbereich Mathematik, Universität Duisburg-Essen, Lotharstr. 65, 47057 Duisburg, Germany (sergio.conti@uni-due.de). This author was supported by the Deutsche Forschungsgemeinschaft through the Schwerpunktprogramm 1095 *Analysis, Modeling and Simulation of Multiscale Problems.*

‡Graduate Aeronautical Laboratories, California Institute of Technology, 1200 E. California Blvd., Pasadena, CA 91101 (patrice.hauret@fr.michelin.com, ortiz@aero.caltech.edu). These authors were supported by the Department of Energy through Caltech's ASCI ASAP Center for the Simulation of the Dynamic Response of Materials.

space and time length scales through a mathematically rigorous determination of laws of effective or macroscopic behavior. The ultimate aim is to formulate parameter- (or "knob"-) free macroscopic models of material behavior based solely on fundamental laws of physics and rigorous approximation theory. However, the practical implementation of this program remains an outstanding challenge of our time in materials science, computational science, and mathematics.

From a mathematical point of view, the formation of deformation microstructure is a manifestation of the phenomenon of *lack of attainment* [24, 49]. Thus, the minimum principles that govern incremental behavior involve functionals that are often nonconvex and lack lower semicontinuity, with the result that their infimum is not attained by any classical solution. The infimum can nevertheless be approached arbitrarily close by sequences of fields that exhibit increasingly fine microstructure, or *minimizing sequences*. These sequences give mathematical expression to the concept of microstructure. Therefore, the central computational problem concerns the calculation of solutions that exhibit very fine oscillations on the scale of the domain of analysis.

We emphasize that, for the problems under consideration here, the fine oscillations in the solution are the result of material instabilities in an otherwise homogeneous material. Fine oscillations can also be due to oscillatory coefficients in otherwise linear partial differential equations or, more generally, to an oscillatory explicit spatial dependence of the energy density. Problems of this nature are studied within the field of *homogeneization* and are very different in nature from the problems considered in the present work (see, e.g., [19] for a modern treatment of the subject).

For problems such as nonlinear elasticity or plasticity whose energies are invariant under rescaling of the domain, thus resulting in a strict separation of the microscopic and macroscopic length scales, the standard mathematical device for the solution of multiscale problems is *relaxation* [34, 35, 24, 25, 49, 9]. The process of relaxation produces a new effective or "relaxed" problem that is well-posed in the sense of existence of solutions and that implicitly accounts for the formation of microstructure. Indeed, the relaxed problem is fashioned by identifying *optimal microstructures*, i.e., minimizing sequences of fields whose energies converge to the infimum of the energy. Conversely, optimal microstructures can be reconstructed, with no loss of information, from the solutions of the relaxed problem, which, however, are themselves free of fine oscillations.

The finite element method provides an ideal framework for the implementation of the method of relaxation: the oscillation-free solutions of the relaxed problem are approximated by finite element interpolation; and microstructure is accounted for at the *subgrid* level. Such schemes conform to the *concurrent* multiscale computing paradigm in that both the macroscopic solution and the attendant microstructures are computed *simultaneously* as part of the same calculation. The earliest realizations of this general strategy were concerned with the effective simulation of shear bands resulting from unstable plastic deformation. To this end, Ortiz et al. (see [52, 43, 45, 50, 44]) embedded a *discontinuous mode* of deformation carrying a strain discontinuity into finite elements, which they treated as *incompatible elements*. The detection of the point of local instability and the orientation of the resulting strain discontinuities were determined by a local Hadamard stability analysis. Numerous variations of this basic scheme were proposed subsequently, and the resulting elements have been generally referred to as *enhanced-strain elements*.

From the standpoint of relaxation, the local strain fields in enhanced-strain elements represent simple microstructures. The precise structure of the strain enhance-

ment is immaterial as regards the effective behavior of the element; only the so-called Young measure generated by the strain enhancement matters. This Young measure keeps track of the volume fractions occupied by the different strains introduced by the local enhancement. This observation was made by Leroy, Ortiz, and Needleman [45], who showed that the original element of Ortiz, Leroy, and Needleman [52] and the embedded-band element of Belytschko, Fish, and Engelmann [7] are indeed identical. In addition, the local Hadamard stability analysis underlying enhanced-strain elements is often based on a linearization of the constitutive relations, leading to the so-called Hill equivalent solid, and the resulting local enhancements fail to fully exploit the strongly nonlinear multiwell structure of the energy landscape.

More general concurrent multiscale computing schemes based on modern calculus of variations tools have been proposed recently [13, 53, 54, 28, 8, 26, 21, 4, 12, 46, 55]. These schemes allow a fully nonlinear analysis of the energy to be performed at the subgrid scale and generate microstructures "on-the-fly" by a variety of algorithms such as sequential lamination [40, 41, 42] and recursive faulting [55]. While this approach conforms strictly to the multiscale modeling paradigm, i.e., it involves no empirical modeling of the macroscopic or effective behavior, the generation of subgrid microstructure requires the solution of a complex nonconvex optimization problem and is often computationally costly. Considerable gains in performance are achieved when the relaxation of the constitutive relations *is known analytically.* Thus, when the relaxation of the problem is known explicitly, the construction of subgrid microstructures is bypassed entirely. However, the behavior of the elements is optimal, i.e., as compliant as possible, and optimal microstructures can be reconstructed a posteriori with no loss of information. Unfortunately, explicit relaxations are known only for a handful of material models, though the list of such models continues to grow at a steady rate.

In this paper we present a rigorous formulation of the concurrent multiscale computing paradigm just described; we establish the connection between concurrent multiscale computing and enhanced-strain elements; and we illustrate the approach in an important area of application, namely, single-crystal plasticity, for which the explicit relaxation of the problem is derived analytically. Our relaxation theorem extends an earlier result of Conti and Ortiz [22] to the hardening case. The paper is organized as follows. Fundamental results of the direct method in the calculus of variations concerning existence of minimizers and relaxation are briefly reviewed in section 2. Section 3 is concerned with the convergence of conforming discrete approximations to the relaxed functional in the nonlinear range. Section 4 discusses relaxation in a model of crystal plasticity. Section 5 is devoted to establishing the connection of enrichment techniques and partial relaxation. Section 6 provides an example of application of the relaxation approach to multiscale computations in single-crystal plasticity. Finally, closing remarks and an outlook are collected in section 7.

2. Infimization and relaxation. For completeness and to set the stage for subsequent developments, we begin by reviewing relevant results of the calculus of variations with particular focus on relaxation of functionals defined on Sobolev spaces (see, for instance, [25, 24, 49] for extensive presentations).

Throughout this work we are concerned with systems whose behavior can be described by means of a minimum principle of the form

$$\inf_{u\in X} J(u), \tag{2.1}$$

where X is a metric space (a topological space would suffice for most results, see [25],

but we shall not require such generality) and $J : X \to \overline{\mathbb{R}} \equiv \mathbb{R} \cup \{\pm\infty\}$ is a functional defined over X. In applications, X will be a subset of a Sobolev space $W^{1,p}(\Omega;\mathbb{R}^n)$. The direct method of the calculus of variations permits us to establish existence of minimizers of J over X by establishing that any minimizing sequence, i.e., any sequence $u_i \in X$ such that $J(u_i) \to \inf_X J$, has a subsequence that converges to a minimum. The key properties of the functional that result in existence are coercivity and lower semicontinuity. We recall that a functional J is coercive in X if for any $t \in \mathbb{R}$ the closure of the set $\{J \leq t\} \equiv \{v \in X,\ J(v) \leq t\}$ is compact in X. In addition, J is said to be lower semicontinuous if for every $u \in X$ and every sequence $u_i \to u$ it follows that $J(u) \leq \liminf_{i\to\infty} J(u_i)$. Coercivity immediately implies that any sequence u_i for which $J(u_i)$ is bounded has a subsequence converging to some $u \in X$. The final step is then to show that the limit minimizes J. In order to do so it suffices to prove that $J(u) \leq \liminf_{i\to\infty} J(u_i) = \inf J$, which is implied by lower semicontinuity of J.

In the present work we are concerned with functionals, such as those describing materials which spontaneously generate microstructure, lacking lower semicontinuity and in their relaxation. A key notion in the theory of relaxation is that of *lower semicontinuous envelope*. The lower semicontinuous envelope $\mathrm{sc}^- J : X \to \overline{\mathbb{R}}$ of J is defined as the supremum of all lower semicontinuous functionals majorized by J, i.e., $\mathrm{sc}^- J(u) = \sup\big\{G(u)$ such that $G : X \to \overline{\mathbb{R}}$ lower semicontinuous, $G(v) \leq J(v)$ for all $v \in X\big\}$. It is easy to see that $\mathrm{sc}^- J$ is lower semicontinuous and

$$\mathrm{sc}^- J(u) = \inf\left\{\liminf_{i\to\infty} J(u_i) : u_i \in X\,,\ u_i \to u\right\}\,. \tag{2.2}$$

For any coercive functional J the following hold [25, p. 30]:

1. $\mathrm{sc}^- J$ is coercive and lower semicontinuous.
2. $\mathrm{sc}^- J$ admits at least a minimum point.
3. $\min_{u\in X} \mathrm{sc}^- J(u) = \inf_{u\in X} J(u)$.
4. If u is the limit of a minimizing sequence for J, then u is a minimum point for $\mathrm{sc}^- J$.
5. If u is a minimum point for $\mathrm{sc}^- J$, then u is the limit of a minimizing sequence of J.

These properties establish a close and rigorous connection between minimum problems and their relaxations. Thus, whereas the original problem may suffer from non-attainment, the relaxed problem always has solutions. In addition, solving the relaxed problem is equivalent to solving the original problem in as much as the macroscopic or structural behaviors (e.g., energies, force-displacement relations) computed from both problems are identical; and the solutions (minimizers) of the relaxed problem are in one-to-one correspondence to solutions (minimizing sequences) of the original problem.

Throughout this work we restrict our attention to functionals J of the integral form

$$J(u) = \int_\Omega W(Du(x))\,dx \qquad \forall u \in X, \tag{2.3}$$

where $\Omega \subset \mathbb{R}^n$ is a Lipschitz domain, Du denotes the weak derivative of u, and

$$X = \{v \in W^{1,p}(\Omega;\mathbb{R}^m), \qquad v = 0 \text{ on } \Gamma_D\}, \qquad 1 < p < +\infty. \tag{2.4}$$

Here $\Gamma_D \subset \partial\Omega$ is the part of the boundary of Ω on which Dirichlet or displacement boundary conditions are imposed. Even with strong growth conditions on W,

these functionals are not coercive with respect to the norm topology. However, the functionals can be coercive with respect to the weak topology. We recall that for $1 < p < \infty$ a sequence $(f_i)_{i\in\mathbb{N}}$ in $L^p(\Omega;\mathbb{R}^m)$ converges weakly to $f \in L^p(\Omega;\mathbb{R}^m)$, $f_i \rightharpoonup f$, if $\lim_{i\to\infty} \int_\Omega f_i \cdot g = \int_\Omega f \cdot g$, for every $g \in L^{p'}(\Omega;\mathbb{R}^m)$, where $p' = p/(p-1)$. Analogously, a sequence $(u_i)_{i\in\mathbb{N}}$ converges to u weakly in $W^{1,p}(\Omega;\mathbb{R}^m)$ if u_i converges weakly to u in $L^p(\Omega;\mathbb{R}^m)$, and Du_i converges weakly to Du in $L^p(\Omega;\mathbb{R}^{m\times n})$.

The main property of weak convergence of interest here is that bounded sequences have weakly converging subsequences. More precisely, since the spaces $W^{1,p}$ for $1 < p < \infty$ are separable and reflexive, any bounded subset is compact with respect to the weak topology [57]. Furthermore, we recall that bounded subsets of $W^{1,p}$ are metrizable in the weak topology [57, Theorem 3.16] and, hence, for present purposes it suffices to consider metric spaces. In this setting, the coercivity of J simply expresses the property that its sublevel sets are bounded in $W^{1,p}$.

The coercivity of the functional J can be determined from the growth of W. Precisely, if for some $1 < p < \infty$ we have

$$\frac{1}{C}|F|^p - C \le W(F) \qquad \forall F \in \mathbb{R}^{m\times n}\,, \tag{2.5}$$

then it follows that

$$\frac{1}{C}\int_\Omega |Du|^p \le J(u) + C|\Omega|\,.$$

Hence Du is bounded in $L^p(\Omega;\mathbb{R}^{m\times n})$ whenever J is bounded. If additionally the set Γ_D has positive $n-1$-dimensional measure, then by the Poincaré–Wirtinger inequality u is also bounded in $L^p(\Omega;\mathbb{R}^m)$. Hence u is bounded in $W^{1,p}$, which establishes the coercivity of J in the weak $W^{1,p}$ topology.

Equation (2.5) shows that coercivity depends only on the behavior of W at infinity. Weak lower semicontinuity instead depends on the behavior of W on the entire space of matrices. In one spatial dimension weak lower semicontinuity is equivalent to convexity of the energy density W. In general, weak lower semicontinuity of the energy J given by (2.3) is closely related to the notion of *quasiconvexity* introduced by Morrey [47, 48]. We recall that $W : \mathbb{R}^{m\times n} \to \mathbb{R}$ is quasiconvex if for every open bounded domain $\omega \subset \mathbb{R}^n$,

$$\int_\omega W(F + Dv) \ge \int_\omega W(F) \qquad \forall v \in W_0^{1,\infty}(\omega;\mathbb{R}^m)\,. \tag{2.6}$$

The relation between quasiconvexity and lower semicontinuity is as follows (cf., e.g., [49, Theorem 4.4]).

THEOREM 2.1. *Let $W : \mathbb{R}^{m\times n} \to \mathbb{R}$ be continuous, and assume that there exists a constant $C > 0$ and $1 < p < \infty$ such that*

$$0 \le W(F) \le C(1 + |F|^p) \qquad \forall F \in \mathbb{R}^{m\times n}. \tag{2.7}$$

In addition, let $\Omega \subset \mathbb{R}^n$ be a bounded Lipschitz domain. Then J defined by (2.3) *is weakly lower semicontinuous on $W^{1,p}(\Omega;\mathbb{R}^m)$ if and only if W is quasiconvex.*

If W is not quasiconvex, and correspondingly J not lower semicontinuous, the *quasiconvex envelope* of W determines the lower semicontinuous envelope of J. Precisely, the following holds [24, Theorem 2.1, p. 228], [49, Theorem 4.5].

THEOREM 2.2. *Let $J : X \to \overline{\mathbb{R}}$ be the functional defined in* (2.3), (2.4). *Let $W : \mathbb{R}^{m\times n} \to \mathbb{R}$ be continuous and such that*

$$\frac{1}{C}|F|^p - C \le W(F) \le C + C|F|^p \qquad \forall F \in \mathbb{R}^{m\times n}, \tag{2.8}$$

for some $1 < p < +\infty$ and $C > 0$. Then the lower semicontinuous envelope of J in weak topology of $W^{1,p}(\Omega;\mathbb{R}^m)$ is given by

$$\mathrm{sc}^- J(u) = \int_\Omega \mathcal{Q}W(Du)\,, \tag{2.9}$$

where $\mathcal{Q}W : \mathbb{R}^{m\times n} \to \mathbb{R}$ denotes the quasiconvex envelope of W, which can be computed as

$$\mathcal{Q}W(F) = \inf_{v\in W_0^{1,\infty}(\omega;\mathbb{R}^m)} \frac{1}{|\omega|}\int_\omega W(F + Dv) \qquad \forall F \in \mathbb{R}^{m\times n}. \tag{2.10}$$

Expression (2.10) *is independent of the choice of the open bounded domain $\omega \subset \mathbb{R}^n$, provided that its boundary has zero Lebesgue measure.*

In scalar or one-dimensional problems (i.e., if $m = 1$ or $n = 1$) the quasiconvex envelope coincides with the convex envelope, which is easily computable. In general, the computation of quasiconvex envelopes is exceedingly difficult, and explicit relaxations are known only for a handful of material models. Representative examples include the following.

Example 2.1 (Pipkin's formula). Consider functions W of the form

$$W(F) = \overline{W}(F^\top F) \qquad \forall F \in \mathbb{R}^{m\times n},$$

with $\overline{W}$ convex and $m \ge n$. An explicit formula for $\mathcal{Q}W$ was obtained by Pipkin [56] in the case $m > n$ and extended by Le Dret and Raoult [29] to the case $m = n$. The result is

$$\mathcal{Q}W(F) = \inf_{S\in\mathbb{S}^+_n} \overline{W}(F^\top F + S) \qquad \forall F \in \mathbb{R}^{m\times n}, \tag{2.11}$$

where $\mathbb{S}^+_n$ is the set of symmetric semidefinite positive matrices in $\mathbb{R}^{n\times n}$. Le Dret and Raoult have also shown that formula (2.11) does not hold for $m < n$. ∎

Example 2.2 (liquid-crystal elastomers). Liquid-crystal elastomers display a number of interesting mechanical and optical properties due to the coupling between the liquid-crystal ordering phase transition and rubber elasticity. Presence of the phase transition leads to nonquasiconvexity of the energy and to microstructure formation. The explicit computation of the quasiconvex envelope of the energy by DeSimone and Dolzmann [26] in the isotropic model permitted efficient macroscopic finite element simulations [21]. For a more refined anisotropic model, including an anisotropy term, the relaxation could be obtained only in two dimensions [20]; numerical simulations were then performed for a membrane geometry. The microstructure could be locally reconstructed by inverting the quasiconvexification procedure. Comparison with experiment showed very good agreement with both macroscopic and microscopic properties computed through the relaxed functional, in particular for the anisotropic model. The quasiconvex envelope of the anisotropic model in three dimensions remains unknown at present. ∎

Example 2.3 (sequential faulting in confined brittle samples). When fractures arise in confined brittle materials, distributed damage instead of localized isolated cracks can be expected (cf. the experiments of Chen and Ravichandran [16, 17, 14, 15]). Such a distribution of damage can be understood as the occurrence of microstructure, and the energy to be minimized indeed lacks lower semicontinuity. In order to provide numerical partial relaxation, Pandolfi, Conti, and Ortiz [55] propose to introduce distributions of cracks, or recursive-faulting, which share several characteristics with—but also differs in significant respects from—sequential lamination. In the particular case of purely cohesive frictionless fracture, the sequential faulting construction can be shown to deliver the relaxation of the energy [55]. The relaxed energy exhibits a marked tension-compression asymmetry. Thus, whereas in hydrostatic tension the fault microstructure is capable of fully relaxing the energy, under hydrostatic tension—or "confinement"—the microstructure can only relax shear and the material behaves as a compressible fluid in hydrostatic equilibrium. □

Crystal plasticity is also amenable to analytical relaxation. This relaxation is discussed in detail in section 4.

3. Convergence of approximations. In this section we consider successive approximations of infima over increasingly finer conforming finite element spaces $(X_i)_{i\geq 0} \subset X$. Under natural assumptions we show that subsequences of successive minima over X_i, $i \geq 0$, converge to minima of the relaxed energy $\mathrm{sc}^- J$ as $i \to \infty$. While the arguments that we use are based on standard theory of Γ-convergence (cf., e.g., [34, 35, 25, 9]), they are not widely known in the finite element literature and will, therefore, stand a brief exposition.

3.1. Elements of Γ-convergence. Let $(J_i)_{i\in\mathbb{N}}$ be a sequence of functionals from X to $\overline{\mathbb{R}}$. We recall that J_i Γ-converges to $J : X \to \overline{\mathbb{R}}$ if the following two properties hold:

1. For every $u \in X$, and every sequence $u_i \to u$,
$$J(u) \leq \liminf_{i\to\infty} J_i(u_i).$$
2. For every $u \in X$, there is a sequence $u_i \to u$ such that
$$J(u) = \lim_{i\to\infty} J_i(u_i)\,.$$

The Γ-limit J is automatically lower semicontinuous. Furthermore, a constant sequence $J_i = J$ always has a Γ-limit, namely, the lower semicontinuous envelope $\mathrm{sc}^- J$ of J.

Extension of the direct method to a family of functionals requires a uniform coercivity assumption. We recall a sequence $(J_i)_{i\in\mathbb{N}}$ is equicoercive in X if for any $t \in \mathbb{R}$ there exists a compact set $K_t \subset X$ independent of i such that for all $i \in \mathbb{N}$, $\{u \in X,\, J_i(u) \leq t\} \subseteq K_t$.

Consider now an equicoercive sequence J_i Γ-converging to a functional J. Then J is coercive. Since in addition Γ-limits are lower semicontinuous, it immediately follows that the Γ-limit of any equicoercive sequence has a minimizer. Furthermore, their minimizers are accumulation points of minimizing sequences of the family J_i. Precisely, if $J_i(u_i) = \inf J_i$, then the sequence u_i has a subsequence that converges to a minimizer of J. The converse cannot be true, since J_i need not have a minimizer. It is, however, true if approximate minimizers are considered. Assume for definiteness that $J_i \geq 0$ and J is not identically $+\infty$. Then the set of minimizers of J coincides

with the set of accumulation points of the set of minimizing sequences *of the family* J_i, i.e., $\{u : J(u) = \inf J\}$ = accumulation points of $\{u_i : \lim_{i\to\infty} [J_i(u_i) - \inf J_i] = 0\}$.

3.2. Approximation and convergence analysis in the conforming case. Let $(X_i)_{i\in\mathbb{N}} \subset X$ be a sequence of finite-dimensional approximation spaces.

DEFINITION 3.1. *A sequence of sets $(X_i)_{i\in\mathbb{N}} \subset X$ is dense in X if for any $u \in X$, there exists a sequence $(u_i)_{i\in\mathbb{N}}$ converging to u in X such that $u_i \in X_i$ for every $i \in \mathbb{N}$.*

Under certain restrictions on the approximation of the domain, conforming finite element spaces, such as those generated by piecewise affine interpolation, on increasingly finer meshes define dense sequences in the sense of (3.1) (cf. [18]).

In what follows, we denote by (X, T) and (X, S) the space X endowed with the strong (T) and with the weak topology (S), respectively. Whereas first-countability assumption would suffice in most cases, for the applications under consideration here we may assume all topologies to be metrizable without loss of generality. We recall that the topology T is finer than S; i.e., any converging sequence for T converges for S.

PROPOSITION 3.2. *The set X is assumed to be endowed with two metrizable topologies S and T, with T finer than S. Let $J : X \to \overline{\mathbb{R}}$ be coercive in (X, S) and continuous in (X, T). Let $(X_i)_{i\in\mathbb{N}} \subset X$ be a dense sequence of sets in (X, T) and $(J_i)_{i\in\mathbb{N}} : X \to \overline{\mathbb{R}}$ be the sequence defined by*

$$J_i(u) = \begin{cases} J(u) & \text{if } u \in X_i, \\ +\infty & \text{otherwise,} \end{cases} \tag{3.1}$$

for every $i \in \mathbb{N}$ and every $u \in X$. Then the sequence $(J_i)_{i\in\mathbb{N}}$ Γ-converges to $\mathrm{sc}^- J$ in (X, S) and is equicoercive in (X, S). Here $\mathrm{sc}^- J$ is the lower semicontinuous envelope of J in (X, S).

Proof. Let $u \in X$, and $u_i \to u$, with respect to S. Since $J_i \geq J$ on X for every $j \in \mathbb{N}$, we have

$$\mathrm{sc}^- J(u) \leq \liminf_{i\to\infty} J(u_i) \leq \liminf_{i\to\infty} J_i(u_i)\,. \tag{3.2}$$

This proves the first inequality in the definition of Γ-convergence. Let now $u \in X$. By (2.2) there is a sequence $u^k \to u$ in S such that

$$\lim_{k\to\infty} J(u^k) = \mathrm{sc}^- J(u)\,.$$

By the density of the sequence X_i, for any k there is a sequence $u_i^k \in X_i$, with $u_i^k \to u^k$ with respect to T. Since J is continuous in the same topology, and $J_i = J$ on X_i,

$$\lim_{i\to\infty} J_i(u_i^k) = \lim_{i\to\infty} J(u_i^k) = J(u^k)\,.$$

The proof of Γ-convergence is then completed by passing to a diagonal subsequence.

Since, by construction, $J_i \geq J$, the equicoercivity of the sequence is immediate from the coercivity of J. As noted earlier, this implies that the minimizers of J are accumulation points of minimizing sequences of the family J_i; i.e., if $J_i(u_i) = \inf J_i$, then the sequence u_i has a subsequence that converges weakly to a minimizer of J. ∎

Assume, for instance, that J is of the form (2.3) with $W : \mathbb{R}^{m\times n} \to \mathbb{R}$ continuous and such that

$$c|F|^p - C \le W(F) \le C(1 + |F|^p) \qquad \forall F \in \mathbb{R}^{m\times n}\,, \tag{3.3}$$

for some c, $C > 0$, $p \in (1, \infty)$. As noted earlier, if Ω is a bounded Lipschitz domain, and $\Gamma_D \subset \partial\Omega$ has positive $n-1$-dimensional measure, then J is coercive in the weak topology of $W^{1,p}$. Furthermore, by Lebesgue's dominated convergence theorem J is continuous in the strong topology of $W^{1,p}$. Therefore, Proposition 3.2 applies for any dense sequence $X_i \in W^{1,p}$, e.g., for sequences of spaces generated by conforming finite element interpolation.

4. Application to crystal plasticity. Ductile single crystals develop a variety of fine microstructures when subjected to monotonic or cyclic deformations (see, e.g., [53] for a review). Within a deformation theory of plasticity framework, those deformation microstructures may be understood as the result of the lack of lower semicontinuity conferred on the energy functional by strong latent hardening [53]. Thus, single crystals supply a convenient and nontrivial example of application—as well as an exacting test—of multiscale analysis. Conti and Ortiz have obtained an explicit relaxation of single-crystal plasticity in the limiting case of ideally plastic crystals with infinite latent hardening. In this section, we strengthen Conti and Ortiz's result by extending it to materials exhibiting finite latent hardening and self-hardening.

4.1. Deformation theory of crystal plasticity. Let $\Omega \subset \mathbb{R}^3$ represent the reference configuration of a ductile single crystal, and denote by u the displacement field. Under the hypothesis of small deformations, we adopt the following additive decomposition of the gradient $\beta = Du$ into an elastic and a plastic contribution: $\beta = Du = \beta^e + \beta^p$. We note that β needs to be a gradient field, i.e., $\nabla \times \beta = 0$; this does not necessarily hold for the individual components β^e and β^p. Plastic deformation in single crystals is crystallographic in nature and, for monotonic deformation, the plastic contribution β^p can be expressed as

$$\beta^p(\gamma) = \sum_{i=1}^{N} \gamma_i\, s_i \otimes m_i.$$

The single crystal has N slip systems characterized by the slip directions $(s_i)_{1\le i\le N}$ and the normal vectors $(m_i)_{1\le i\le N}$, the plastic state of the crystal being described by the set of plastic variables $(\gamma_i)_{1\le i\le N}$. Plastic deformations are assumed to be isochoric ($s_i \cdot m_i = 0$ for all $1 \le i \le N$). For example, in fcc crystals one has $N = 12$ and the set of slip systems $\mathcal{S} = \{s_i \otimes m_i;\, 1 \le i \le N\}$ is given by

$$\mathcal{S}_{\text{fcc}} = \big\{(0,1,1) \otimes (\pm 1,1,-1),\ (0,1,-1) \otimes (\pm 1,1,1),\ \text{and cyclic permutations}\big\}\,;$$

for bcc crystals one instead has $N = 24$ and

$$\begin{aligned}\mathcal{S}_{\text{bcc}} = \big\{&(\pm 1,1,1) \otimes (0,1,-1),\ (\pm 1,1,-1) \otimes (0,1,1),\\ &(1,-1,\mp 1) \otimes (2,1,\pm 1),\ (1,1,\mp 1) \otimes (2,-1,\pm 1),\ \text{and cyclic permutations}\big\}\,.\end{aligned}$$

The deformation-theory energy density corresponding to a displacement gradient β and plastic slip strains $\gamma \in \mathbb{R}^N$ can be written as

$$A(\beta,\gamma) = \frac{1}{2}\,(\beta^{\text{sym}} - [\beta^p(\gamma)]^{\text{sym}})\, C\, (\beta^{\text{sym}} - [\beta^p(\gamma)]^{\text{sym}}) + W^p(\gamma)\,,$$

where C is the tensor of elastic moduli of the crystal and the effective stored-energy function $W^p : \mathbb{R}^N \to [0,\infty]$ contains hardening and dissipation terms. The plastic slip-strain field $\gamma : \Omega \to \mathbb{R}^N$ enters the energy locally and, therefore, can be minimized locally. The resulting energy density is

$$W(\beta) = \min_{\gamma\in\mathbb{R}^N} A(\beta,\gamma)\,. \tag{4.1}$$

This deformation-theory energy density defines a minimization problem of the form (2.1) with the functional $J(u)$ defined by (2.3) and (4.1). The properties of the resulting problem depend sensitively on the assumed form of the stored-energy function $W^p(\gamma)$.

4.2. Relaxation of hardening crystal plasticity. The analysis of Conti and Ortiz [22] is concerned with the particular case of ideally plastic crystals with infinite latent hardening, corresponding to the choice of stored-energy density

$$W^p_\infty(\gamma) = \begin{cases} \tau_i\,|\gamma_i| & \text{if } \gamma_j = 0\,\forall\, j \neq i, \\ +\infty & \text{otherwise,} \end{cases} \tag{4.2}$$

where $\tau_i > 0$ are the critical resolved shear stresses of the different slip systems. This stored-energy density effectively rules out multislip deformation at a material point. Its convex envelope is

$$[W^p_\infty]^{**}(\gamma) = W^p_0(\gamma) \equiv \sum_i \tau_i\,|\gamma_i|,$$

which describes multislip ideal plasticity, i.e., crystals that are entirely devoid of latent hardening. Conti and Ortiz [22] showed that under certain kinematic assumptions on the set of slip systems the energy W^p_0 also coincides with the quasiconvex envelope of W^p_∞, thus providing an explicit relaxation of ideally plastic crystals with infinite latent hardening.

We proceed to show that a similar result holds for crystals with arbitrary hardening characteristics. We remark that, as in classical works on geometrically linear plasticity [59, 2, 60], the natural space in which coercivity is achieved is $X \equiv \{u \in BD(\Omega;\mathbb{R}^3);\ \operatorname{div} u \in L^2(\Omega)\}$. We recall that BD is the space of functions of bounded deformation, i.e., the set of L^1 functions such that the symmetric part of the distributional gradient is a bounded measure [59, 2, 60, 1]:

$$\begin{aligned} &BD(\Omega) \\ &\equiv \left\{ u \in L^1(\Omega;\mathbb{R}^3) \text{ s.t. } \sup\left\{ \left| \int_\Omega u\otimes\nabla\phi + \nabla\phi\otimes u \right| : \phi \in C^1_0(\Omega;\mathbb{R}^3) \right\} < \infty \right\}. \end{aligned}$$

We recall that, much as in the case of BV functions, the symmetrized distributional gradient of any function $u \in BD$ can be decomposed as follows:

$$Eu \equiv \frac{Du + (Du)^T}{2} = \mathcal{E}u\,dx + E^s u\,.$$

Here Du is the (matrix-valued) distributional gradient of u; $\mathcal{E}u$ the absolutely continuous part of Eu with respect to the Lebesgue measure; and E^s the rest. In turn, E^s can be decomposed into a part which is absolutely continuous with respect to the

2-dimensional Hausdorff measure $\mathcal{H}^2$ (one dimension less than the space, in general), and which represent jumps in u, and a remainder, called Cantor part. In addition, the relevant topology is the weak topology of U, i.e., weak convergence of u in BD and weak convergence of $\operatorname{div} u$ in L^2. Analogously to the case of Sobolev spaces, on bounded sets this is equivalent to the strong L^1 topology, which is metrizable. Hence we shall use the latter.

THEOREM 4.1. *Let $\Omega \subset \mathbb{R}^3$ be a bounded Lipschitz set and let the set of slip systems $\{s_i \otimes m_i;\ 1 \le i \le N\}$ be $\mathcal{S}_{\mathrm{bcc}}$ or $\mathcal{S}_{\mathrm{fcc}}$. Assume that stored-energy density $W^p : \mathbb{R}^N \to [0,\infty]$ satisfies the inequalities*

$$W_0^p(\gamma) \le W^p(\gamma) \le W_\infty^p(\gamma) \qquad \forall \gamma \in \mathbb{R}^N\,, \tag{4.3}$$

and let W be as in (4.1). *Then the relaxation of the functional $J : X \to [0,\infty]$ defined by*

$$J(u) = \begin{cases} \displaystyle\int_\Omega W(Du) & \text{if } u \in W^{1,2}(\Omega;\mathbb{R}^3), \\ +\infty & \text{otherwise,} \end{cases}$$

with respect to the strong L^1 topology is

$$\mathcal{J}(u) = \begin{cases} \displaystyle\int_\Omega W^{**}(\mathcal{E}u)\,dx + \int_\Omega W^\infty\left(\frac{E_s u}{|E_s u|}\right) d|E_s u| & \text{if } u \in X, \\ +\infty & \text{otherwise.} \end{cases} \tag{4.4}$$

Here W^{**} denotes the convex envelope of W and is obtained from W by replacing the plastic energy W^p by its convex hull $[W^p]^{**} = W_0^p$. In addition, the corresponding regression function follows as $W^\infty(F) = \lim_{t\to\infty} W^{**}(t\,\beta)/t$.

Proof. Let J^∞ denote the functional obtained in the case $W^p = W_\infty^p$. In [22, Theorem 3.3] it was shown that $\mathrm{sc}^- J^\infty = \mathcal{J}$, with respect to the strong L^1 topology. This implies, in particular, that $\mathcal{J}$ is lower semicontinuous. We claim that $\mathcal{J}(u) \le J(u)$ for all u. Since the right-hand side is ∞ for $u \notin W^{1,2}$, it suffices to consider the case $u \in W^{1,2}$. But then $\mathcal{J}(u)$ equals the integral of $W^{**}(\nabla u)$, and since by assumption $W^{**} = W_0^p \le W^p$, the claim follows. From the definition of the lower semicontinuous envelope it follows that

$$\mathcal{J} \le \mathrm{sc}^- J\,. \tag{4.5}$$

We now prove the converse inequality. By [22, Theorem 3.3] for any $u \in X$ there is a sequence $u_i \in W^{1,2}(\Omega;\mathbb{R}^3)$ such that $u_i \to u$ in L^1, and $J^\infty(u_i) \to \mathcal{J}(u)$. Since $J \le J^\infty$, we have

$$\limsup_{i\to\infty} J(u_i) \le \limsup_{i\to\infty} J^\infty(u_i) = \mathcal{J}(u)\,.$$

In turn, $\mathrm{sc}^- J$ is lower semicontinuous and below J, and hence

$$\mathrm{sc}^- J(u) \le \liminf_{i\to\infty} \mathrm{sc}^- J(u_i) \le \limsup_{i\to\infty} \mathrm{sc}^- J(u_i) \le \limsup_{i\to\infty} J(u_i)\,.$$

Comparing these two relations it is clear that

$$\mathrm{sc}^- J \le \mathcal{J},$$

which, together with (4.5), implies the thesis. ∎

Remark 1. The same proof used in [22] establishes that the relaxation remains unchanged under the addition of certain additional kinematical constraints, including

(i) the slip boundary condition $(u - u_0) \cdot \nu = 0$ prescribed over $\Gamma \subset \partial\Omega$, where ν denotes the normal unit vector on Γ;
(ii) the linearized incompressibility constraint $\operatorname{div} u = 0$. ∎

PROPOSITION 4.2. *If, in addition to* (4.3)*, the stored-energy density W^p satisfies the inequality*

$$W^p(\gamma) \le M|\gamma| \quad \forall \gamma \in \mathbb{R}^N , \tag{4.6}$$

for some $M \in \mathbb{R}$, then Theorem 4.1 *holds for* any *set of slip systems spanning the set of traceless symmetric matrices.*

The key point of the proof is the following extension of Lemma 3.5 of [22].

LEMMA 4.3. *Let $\mathcal{S} = \{s_i \otimes m_i;\ 1 \le i \le N\}$ be a set of slip systems such that their symmetric parts span the set of traceless symmetric matrices. Then there is a constant $c > 0$ such that*

$$W(\beta) \le c(|\beta + \beta^T| + |\operatorname{Tr}\beta|^2)$$

for all $\beta \in \mathbb{R}^{3\times 3}$.

Remark 2. In comparing with Lemma 3.5 of [22], the degenerate laminate $\nu = \delta_\beta$ should be considered. ∎

Proof. Consider the linear map $T : \mathbb{R}^N \to \mathbb{R}^{3\times 3}$ defined by

$$T\gamma = \sum_{i=1}^{N} \gamma_i \frac{s_i \otimes m_i + s_i \otimes m_i}{2} .$$

By assumption, $T\mathbb{R}^N = \mathbb{R}^{3\times 3}_{\mathrm{sym},0}$, where $\mathbb{R}^{n\times n}_{\mathrm{sym},0} = \{F \in \mathbb{R}^{n\times n} : F^T = F,\ \operatorname{Tr} F = 0\}$ is the set of symmetric, traceless matrices. Therefore T has a linear inverse $S : \mathbb{R}^{3\times 3}_{\mathrm{sym},0} \to \mathbb{R}^N$ (not necessarily uniquely defined). Consider now a generic $\beta \in \mathbb{R}^{3\times 3}$, and define

$$\beta^D_{\mathrm{sym}} = \frac{\beta + \beta^T}{2} - \frac{1}{3}(\operatorname{Tr}\beta)\mathrm{Id} \in \mathbb{R}^{3\times 3}_{\mathrm{sym},0} .$$

We set $\gamma = S\beta^D_{\mathrm{sym}}$. Then

$$\beta = \omega + \sum_{i=1}^{N} \gamma_i s_i \otimes m_i + \frac{1}{3}(\operatorname{Tr}\beta)\mathrm{Id} ,$$

with ω antisymmetric, and $|\gamma| \le C|\beta^D_{\mathrm{sym}}| \le C|\beta + \beta^T|$, with a constant depending on $\mathcal{S}$ but not on β. Therefore, recalling (4.6),

$$W(\beta) \le c|\operatorname{Tr}\beta|^2 + |\beta + \beta^T| C \max_i \tau_i ,$$

with a constant depending on the elastic moduli C and on $\mathcal{S}$. The thesis follows. ∎

5. Algorithmic relaxation. In the absence of an explicit knowledge of the relaxed energy, a fall back strategy is to approximate the relaxation by the consideration of *special microstructures*. These microstructures can be evaluated a priori, and the relaxed energy tabulated for subsequent use; or they can be generated "on the fly," simultaneously with the full scale simulation.

5.1. Sequential lamination. Given the variational structure of the problems under consideration, upper bounds are particularly useful: if W is replaced by any function $\tilde{W}$ such that $\mathcal{Q}W \le \tilde{W} \le W$, then $\mathrm{sc}^- J$ is not changed. However, if $\tilde{W}$ is a good approximation to $\mathcal{Q}W$, the numerical behavior of the functional might be largely improved. Practically all available approximations to $\mathcal{Q}W$ from above are obtained through the following result, which is (under slightly more stringent assumptions) due to Morrey [47, 48]. The present version is proven in [31]; see also [49, Lemma 4.3].

LEMMA 5.1. *If $W : \mathbb{R}^{m\times n} \to \mathbb{R}$ is quasiconvex, it is rank-1 convex. This means that for all $A, B \in \mathbb{R}^{m\times n}$ with $\mathrm{rank}(B - A) = 1$, and every $\lambda \in [0, 1]$, one has*

$$W(\lambda A + (1-\lambda)B) \le \lambda W(A) + (1-\lambda)W(B).$$

The converse assertion is false, as proved by the counterexample of Šverák [61]. To characterize the rank-1 convex envelope, we follow the approach of Kohn and Strang [39, 40, 41, 42].

LEMMA 5.2. *Let $W : \mathbb{R}^{m\times n} \to \mathbb{R}$. The rank-1 convex envelope $\mathcal{R}W$ of W, i.e., the greatest rank-1 convex function below W, is characterized for every $F \in \mathbb{R}^{m\times n}$ by $\mathcal{R}W(F) = \lim_{k\to\infty} \mathcal{R}_k W(F)$ with*

$$\begin{aligned}
\mathcal{R}_0 W(F) &= W(F),\\
\mathcal{R}_{k+1} W(F) &= \inf\Big\{ \lambda \mathcal{R}_k W(F_1) + (1-\lambda)\mathcal{R}_k W(F_2) :\ \lambda F_1 + (1-\lambda)F_2 = F,\\
&\qquad \lambda \in [0,1],\ \textit{and } \mathrm{rank}(F_1 - F_2) \le 1 \Big\} \qquad \forall k \in \mathbb{N}^*.
\end{aligned}$$

Additionally, for every $F \in \mathbb{R}^{m\times n}$ and all k, we have $\mathcal{Q}W(F) \le \mathcal{R}W(F) \le \mathcal{R}W_k(F) \le W(F)$.

This iterative characterization is particularly useful if the rank-1 envelope is reached after a *finite number* K of steps, so that $\mathcal{R}W(F) = \mathcal{R}_K W(F)$. This is, however, in general not true; see the discussion accompanying [24, Theorem 1.1, p. 201]. From a numerical point of view, in [27, 28] an algorithm for the global determination of rank-1 convex envelopes has been developed and uniform convergence estimates have been proven.

Due to the computable character of $\mathcal{R}_K W(F)$, it is tempting to replace the quasiconvex envelope $\mathcal{Q}W(F)$, unaccessible in general, by the sequential lamination $\mathcal{R}_K W(F)$, where K is fixed to a small value (typically $K = 1$). Then the energy which will be minimized over finite-dimensional spaces is

$$\int_\Omega \mathcal{R}_K W(Du). \tag{5.1}$$

Of course, the sequentially laminated energy (5.1) is not guaranteed to have a minimum over X, but the approach has proven useful in elastoplasticity [53, 54, 4, 22, 12].

5.2. Local enrichment and partial relaxation. In this section, we illustrate the relation between local enrichment and relaxation in computational hyperelasticity within the finite element framework. Let us consider J of the form (2.3) defined on the space X given by (2.4). We denote by $\mathcal{T}_h$ a mesh of the polygonal domain Ω, and by X_h the associated discrete space of displacements defined as

$$X_h \equiv \{ v \in X,\ v|_T \in [\mathsf{R}_q(T)]^n\ \forall T \in \mathcal{T}_h \}, \tag{5.2}$$

where $\mathsf{R}_q(T)$ is the space of polynomials of total (resp., partial) order less than q on the simplex (resp., parallelepiped) T. For each element $T \in \mathcal{T}_h$, we choose a finite-dimensional space $E_h(T) \subset W_0^{1,\infty}(T;\mathbb{R}^m)$ of local enrichments. The space E_h of enrichments over Ω can then be defined as

$$E_h \equiv \{v \in W^{1,\infty}(\Omega;\mathbb{R}^m),\ v|_T \in E_h(T)\ \forall T \in \mathcal{T}_h\}. \tag{5.3}$$

The enriched space of approximation now being $X_h \oplus E_h$, the discretized minimum problem becomes

$$\begin{aligned}
&\inf_{v_h=\overline{v}_h+v'_h \in X_h \oplus E_h} \int_\Omega W(D\overline{v}_h + Dv'_h) \\
&= \inf_{\overline{v}_h \in X_h} \left(\sum_{T\in\mathcal{T}_h} \inf_{v'_h \in E_h(T)} \left(\int_T W(D\overline{v}_h + Dv'_h) \right) \right) \\
&= \inf_{\overline{v}_h \in X_h} \sum_{T\in\mathcal{T}_h} \mathcal{E}_T W(D\overline{v}_h),
\end{aligned}$$

where we have introduced the *partially relaxed element energy*

$$\mathcal{E}_T W(F) = \inf_{v\in E_h(T)} \int_T W(F+Dv) \qquad \forall F \in L^p(T;\mathbb{R}^{m\times n}). \tag{5.4}$$

Suppose, in particular, that $q = 1$ and, correspondingly, F is piecewise constant, which corresponds to piecewise linear finite element interpolation over simplices. In view of the expression (2.10) for the quasiconvex envelope of W we have

$$\int_T \mathcal{Q}W(F) = \inf_{v\in W_0^{1,\infty}(T;\mathbb{R}^m)} \int_T W(F+Dv) \qquad \forall F \in \mathbb{R}^{m\times n}\,. \tag{5.5}$$

Since $E_h(T) \subset W_0^{1,\infty}(T;\mathbb{R}^m)$ we reach the following conclusion.

PROPOSITION 5.3. *Let T be a simplex, F a constant deformation over T, $E_h(T) \subset W_0^{1,\infty}(T;\mathbb{R}^m)$ a finite-dimensional space of local enrichments, and $\mathcal{E}_T W(F)$ the corresponding partially relaxed local energy,* (5.4)*. Then the following ordering holds:*

$$\int_T \mathcal{Q}W(F) \le \mathcal{E}_T W(F) \le \int_T W(F)\,. \tag{5.6}$$

This proposition implies immediately that if X_h is generated by piecewise linear interpolation, then

$$\inf_{\overline{v}_h\in X_h} \sum_{T\in\mathcal{T}_h} \int_T \mathcal{Q}W(D\overline{v}_h) \le \inf_{\overline{v}_h\in X_h} \sum_{T\in\mathcal{T}_h} \mathcal{E}_T W(D\overline{v}_h) \le \inf_{\overline{v}_h\in X_h} \sum_{T\in\mathcal{T}_h} \int_T W(D\overline{v}_h)\,. \tag{5.7}$$

Under these conditions, the local enrichment of finite element formulations by bubbles as in the variational multiscale method [37, 38] can be interpreted as a partial relaxation of the formulation in the case of minimization problems. Such an approach extends the early ideas of bubble function introduced in [23] and subgrid incompatible modes of [52, 43, 45, 50, 44].

Remark 3. The preceding conclusion is not at odds with the notable improvements provided by local enrichments in problems where lack of lower semicontinuity is not an issue, for instance advection-diffusion problems [32, 10, 33, 11]—which can

also be rewritten as the minimization of a residual in H^{-1} (see [51])—or recovering the *inf-sup* condition for kinematically constrained systems (e.g., incompressibility [3], mortar methods [6, 36]). ∎

Remark 4. We show by means of two counterexamples that the first inequality in Proposition 5.3 does not hold for higher-order elements, not even for convex energy densities. The first example concerns the case $n = m = 1$, with $W(F) = F^2$, so that $\mathcal{Q}W(F) = W(F)$. We take quadratic elements, i.e., $q = 2$, $T = (-1, 1)$, and consider for definiteness the function $\bar{v}_h(x) = x^2$. Then

$$\int_{-1}^{1} \mathcal{Q}W(2x)dx = 2\int_{0}^{1} (2x)^2 dx = \frac{8}{3} > 0\,.$$

However, if $\tilde{v}_j = 1 - x^2 \in E_h$, then

$$\mathcal{E}_T W(F) \leq \int_{-1}^{1} W(\bar{v}_h' + \tilde{v}_j') = \int_{-1}^{1} W(0) = 0\,.$$

For our second example we take $n = 2$, $m = 1$, and $W(F) = (F_1 + F_2)^2 + \varepsilon|F|^2$. This is convex and coercive for any $\varepsilon > 0$, the precise value of which will be chosen at the end. In this case we have $\mathcal{Q}W = W$. Assume $T = (0, 1)^2$, use componentwise affine functions, and let the boundary values be $u(0, 0) = u(0, 1) = u(1, 0) = 0$, $u(1, 1) = 1$. Then the finite element function in T is $u(x) = x_1x_2$, and the corresponding energy is

$$\int_T W(Du) = \int_T \mathcal{Q}W(Du) = \int_T (x_1 + x_2)^2 + \varepsilon(x_1^2 + x_2^2) = \frac{7}{6} + \frac{2}{3}\varepsilon\,.$$

Assume now that the function $v(x) = \min(x_1, x_2) - x_1x_2 \in W_0^{1,\infty}(T)$ is contained in the enrichment set. Then the enriched problem can achieve the energy

$$\int_T W(Du + Dv) = \int_T W(D\min(x_1, x_2)) = \int_T 1 + \varepsilon = 1 + \varepsilon\,.$$

If $\varepsilon < 1/2$, this energy is lower than the one computed above from the quasiconvex envelope. ∎

6. Numerical examples. In this section we present an application of the concurrent multiscale computing methodology described in the foregoing to single-crystal plasticity. Specifically, for computational purposes we take advantage of the knowledge of the exact relaxed energy $\mathrm{sc}^- J = \mathcal{J}$ given by Theorem 4.1. The discretization should be chosen in order to match the functional form, and the coercivity, of $\mathrm{sc}^- J$. As is evident from the expression given in Theorem 4.1, the functional $\mathrm{sc}^- J$ is finite not only on continuous deformations, but also on those with jump discontinuities, and with a distributed singular part in the gradient. Precisely, the singular part $E_s u$ of the strain is the sum of a jump term $E_j u = [u] \otimes n\, \delta_{\mathcal{S}}$ distributed over a 2-dimensional manifold $\mathcal{S}$ inside Ω and a Cantor part $E_c u$ (see [1]), which is difficult to represent. Here, instead, we work with continuous discretizations. Since smooth functions are dense in BD, this choice of interpolation suffices to achieve the relaxation of the functional.

The particular problem under consideration concerns the indentation of a (100) surface of a bcc crystal; see Figure 1. For simplicity, the elastic moduli of the crystal are assumed to be isotropic with Young's modulus $E = 2000$ MPa and Poisson's

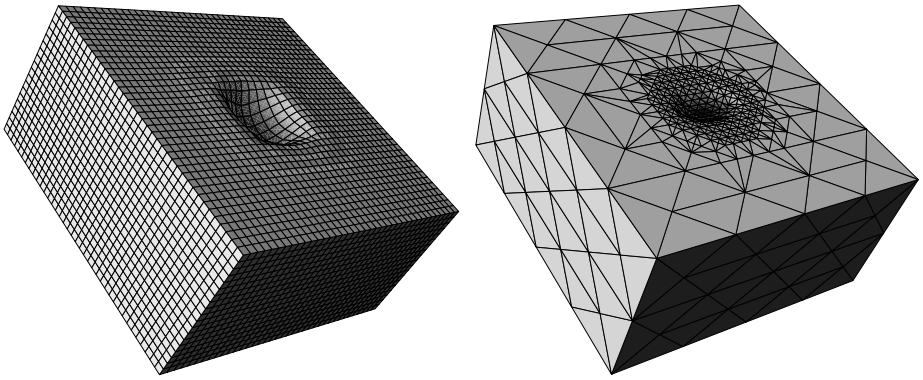

(a) (b)

FIG. 1. *Two models of a bcc single crystal deforming under a rigid indentor.* (a) *hexahedral mesh with* 32000 *nodes,* 27436 *elements;* (b) *tetrahedral mesh with* 5424 *nodes,* 30779 *elements. The vertical displacements are constrained on the base of the crystal, which is otherwise unconstrained.*

ratio $\nu = 0.29$. The crystal is assumed to slip on the $\{211\}[111]$ and $\{110\}[111]$ families of systems, and the critical resolved shear stress is taken to be $\tau_0 = 1.0$ MPa for all systems. Two discretizations of the domain are considered: hexahedral mesh consisting of 32000 nodes and 27436 elements (Figure 1(a)), and a tetrahedral mesh consisting of 5424 nodes and 30779 elements (Figure 1(b)). The vertical displacements are constrained on the base of the crystal, which is otherwise unconstrained.

The computed indentor force/travel curves for the hexahedral and tetrahedral meshes are shown in Figures 2(a) and 2(b), respectively. The figures show the curves computed: in the elastic regime; with the unrelaxed, strong latent hardening, single-crystal plasticity model; with a conventional bubble enhancement [23]; and in the fully relaxed model. As may be seen from the figures, the behavior of the unrelaxed response is much stiffer than the relaxed response, which attains a limit load. The bubble enhancement affords an ostensibly imperceptible gain in compliance with respect to the unrelaxed model.

Finally, we proceed to demonstrate how the optimal microstructures can be reconstructed a posteriori from the solution of the relaxed model. To this end, we begin by recalling the following lemma (for precise definitions of *laminates* as deformation microstructures we refer the reader to [24, 49]; cf. also section 5.1).

LEMMA 6.1 (Lemma 3.6 of [22]). *Under the assumptions of Theorem* 4.1*, for any* $F \in \mathbb{R}^{3\times 3}$ *and any* $\varepsilon > 0$*, there exists a laminate* ν *of finite order such that*

$$\langle \nu, Id\rangle := \int_{\mathbb{R}^{3\times 3}} \beta \, d\nu(\beta) = F,$$

$$\langle \nu, W\rangle := \int_{\mathbb{R}^{3\times 3}} W(\beta)\, d\nu(\beta) \leq W^{**}(F) + \varepsilon,$$

where ν *is understood as a probability measure on the set* $\mathbb{R}^{3\times 3}$ *of matrices.*

Considering that for any $F \in \mathbb{R}^{3\times 3}$ the rank-1 envelope is defined by $\mathcal{R}W(F) = \inf\{\langle \nu, W\rangle;\ \langle \nu, Id\rangle = F\}$, Lemma 6.1 ensures that rank-1 and convex envelopes coincide, i.e., $\mathcal{R}(F) = W^{**}(F)$. Consequently, due to the inequality $\mathcal{R}W \leq \mathcal{Q}W \leq W^{**}$, it follows that the quasiconvex envelope is also equal to the other two,

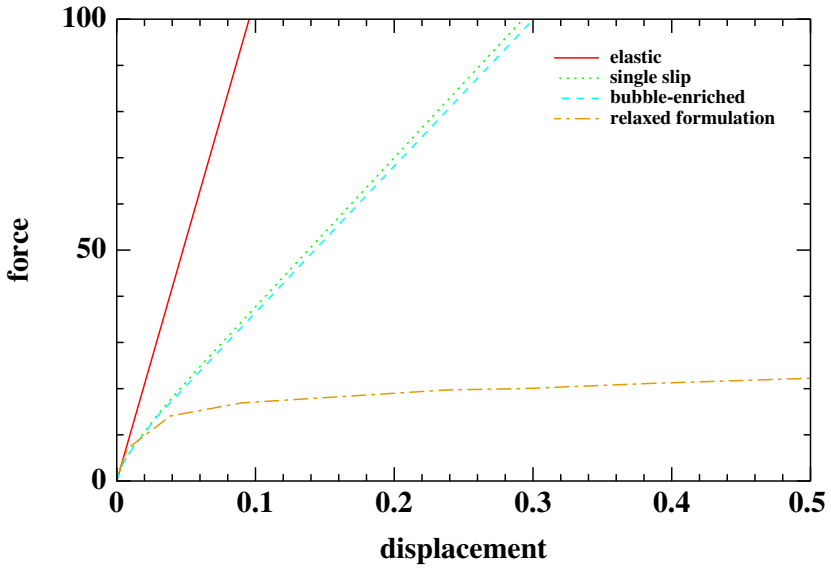

(a)

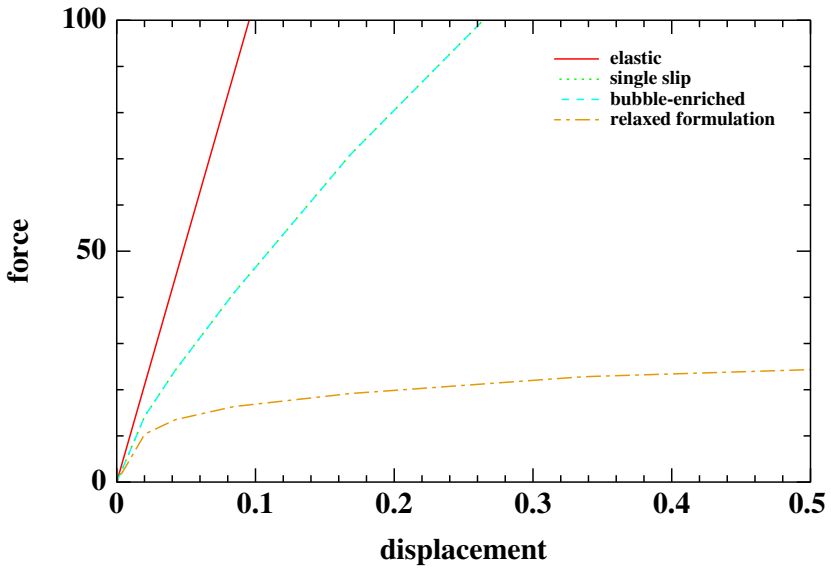

(b)

FIG. 2. *Simulation of bcc single crystal deforming under a rigid indentor. Indentor force/travel displacement curves computed from* (a) *hexahedral mesh;* (b) *tetrahedral mesh. The elastic, single-slip (unrelaxed), relaxed, and bubble-enhanced responses are shown in the figures for comparison.*

$\mathcal{Q}W = \mathcal{R}W = W^{**}$. The proof of Lemma 6.1 given in [22] is based on the explicit construction of the laminate ν. The precise algorithm for reconstructing optimal microstructures from the solutions of the relaxed problem is as follows:

(i) Let $F = F^e + F^p$ be the macroscopic strain. Choose a possible decomposition $F^p = \sum_{i=1}^{I} \gamma_i \, s_i \otimes m_i$. One natural choice criterion to enforce is to make I as small as possible; but in general this does not suffice to make the choice

unique.

(ii) If $0 \leq I \leq 1$, the laminate $\nu = \delta_F$ is satisfactory (even with $\varepsilon = 0$).

(iii) If $I \geq 2$, a recursive construction can be performed. Precisely, assume that a criterion is given to decompose sums of $I-1$ slips into laminates, and consider F as above.

(iii.a) Let $F_1 = F^e + \sum_{i=1}^{I-1} \gamma_i \, s_i \otimes m_i$ and $F_2 = F_1 + \frac{1}{\varepsilon}\gamma_I \, s_I \otimes m_I$, so that $(1-\varepsilon)\,\delta_{F_1} + \varepsilon\,\delta_{F_2}$ is a laminate with average F.

(iii.b) Let $F_3 = F^e + \sum_{i=2}^{I-1} \gamma_i \, s_i \otimes m_i + \frac{1}{\varepsilon}\gamma_I \, s_I \otimes m_I$ and $F_4 = F_3 + \frac{1}{\varepsilon}\gamma_1 \, s_1 \otimes m_1$, so that $(1-\varepsilon)\,\delta_{F_3} + \varepsilon\,\delta_{F_4}$ is a laminate with average F_2.

(iii.c) Compose the two mentioned steps, and obtain the laminate

$$\nu = (1-\varepsilon)\,\delta_{F_1} + \varepsilon(1-\varepsilon)\,\delta_{F_3} + \varepsilon^2\,\delta_{F_4} \tag{6.1}$$

with average F.

(iii.d) F_1 and F_3 involve $I-1$ systems, and hence δ_{F_1} and δ_{F_3} can be replaced by appropriate laminates by the inductive assumption.

The laminate described by (6.1) can be represented by the following tree:

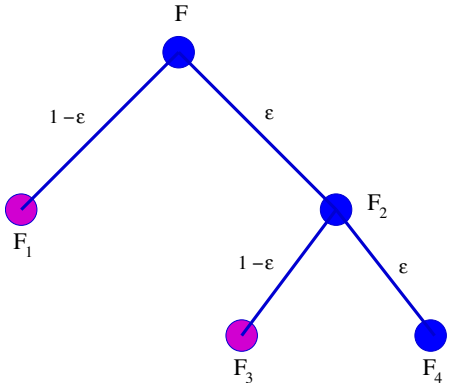

In this diagram each node is the average of its two daughter nodes' weight probabilities specified on the bonds, and each pair of daughter nodes is rank-1 compatible.

Remark 5. It should be carefully noted that the preceding algorithm, while delivering a laminate with the optimal energy (up to an arbitrarily small error ε), it does not always return the simplest possible laminate. In particular, the algorithm never gives a first-order laminate, even when the average plastic strain is the average of a simple laminate supported on two different slip systems (cf. the discussion in section 3.6 of [22], in particular Lemma 3.10). □

It can be shown [22, Lemma 3.5] that there exists a laminate ν_4 such that

$$\langle \nu_4, Id \rangle = F_4, \qquad \langle \nu, W \rangle \leq c(|F_4^{\mathrm{sym}}| + |\mathrm{Tr}\, F_4|^2).$$

Since this part of the laminate involves (as $\varepsilon \to 0$) a negligible volume fraction, and a negligible part of the energy, we do not include it in the visualizations of the microstructures. Additionally, in practice, the slip systems are relabeled such that γ_i increases with $1 \leq i \leq I$. Doing so, our algorithm starts by representing the contribution of the highest components of the plastic variable.

As an illustration of the construction just described, Figures 3 and 4 show the microstructures reconstructed from the solution of the relaxed problem on the hexahedral and tetrahedral meshes, respectively. Each arrow connects a Gauss point to

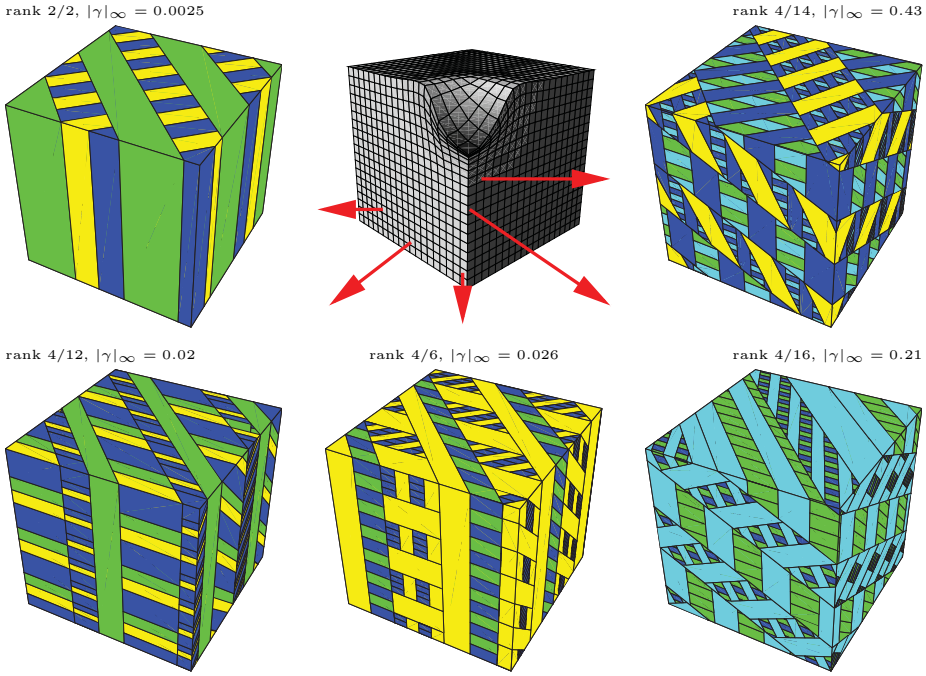

FIG. 3. *Reconstruction at selected Gauss points of optimal microstructures from the solution of the relaxed problem on the hexahedral mesh. All microstructures take the form of sequential laminates. The diagrams represent the interfaces and volume fractions corresponding to all levels of lamination. Each of the resulting regions, or "variants," at the lowest level of lamination is uniformly deformed in single slip. The order of the laminate as well as the maximum slip-strain magnitude are indicated. The reconstruction is performed for* $\varepsilon = 0.5$.

a visualization of the microstructure computed at that Gauss point. All microstructures take the form of sequential laminates. The software used for the visualization of the laminates is due to Fago [30]. The visualization represents the interfaces and volume fractions corresponding to all levels of lamination. Each of the resulting regions, or "variants," at the lowest level of lamination is uniformly deformed in single slip. The complexity of the optimal microstructures is striking. This complexity makes it unlikely that ad hoc strain enhancements, based on polynomial, trigonometric, or similar representations, may come close to being optimal. Indeed, an enhancement must necessarily account for the physical mechanisms of deformation in order to be effective.

7. Concluding remarks. Concurrent multiscale computing provides a powerful means of accounting for the development of deformation microstructures in situations in which there is a strict separation of scales. In these cases, the macroscopic behavior is accurately described by the relaxed problem, which in turn can be solved numerically by standard methods such as finite elements, and the deformation microstructures take place at the subgrid level. The particular example presented in this paper, concerned with single crystals possessing strong latent hardening, demonstrates the vast effect of microstructure formation on the macroscopic behavior of the sample, e.g., on the force/travel curve of a rigid indentor. Thus, whereas the unrelaxed model results in an overly stiff response, the relaxed model exhibits a proper limit load, as

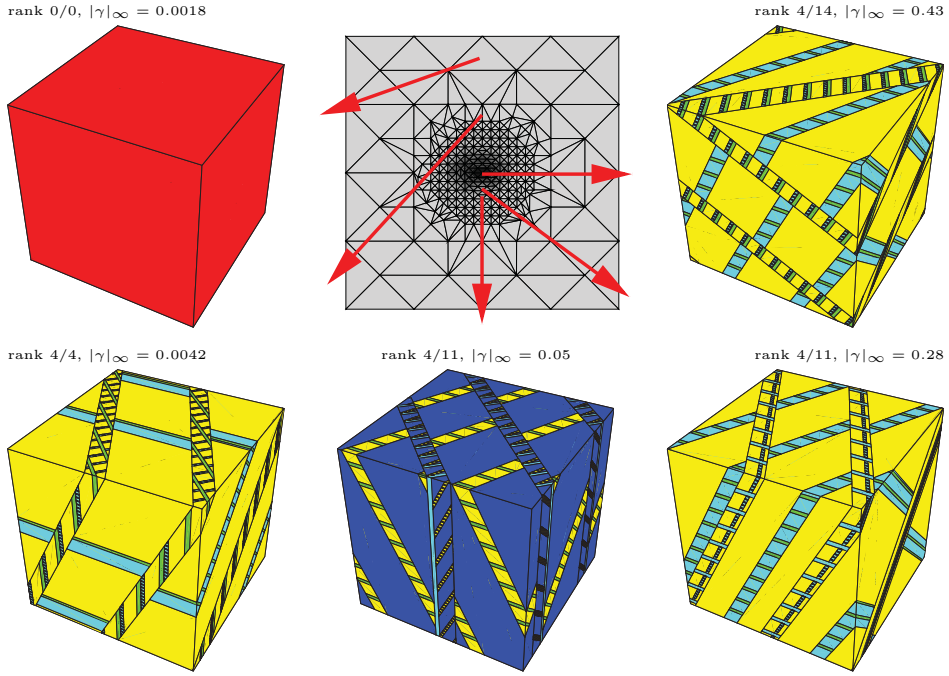

FIG. 4. *Reconstruction at selected Gauss points of optimal microstructures from the solution of the relaxed problem on the tetrahedral mesh. Each arrow connects a Gauss point to a visualization of the microstructure computed at that Gauss point. All microstructures take the form of sequential laminates. The diagrams represent the interfaces and volume fractions corresponding to all levels of lamination. Each of the resulting regions, or "variants," at the lowest level of lamination is uniformly deformed in single slip. The order of the laminate as well as the maximum slip-strain magnitude are indicated. The reconstruction is performed for* $\varepsilon = 0.2$.

expected. The numerical examples reported in this paper also illustrate that ad hoc element enhancements are unlikely to result in any significant relaxation. The application to single crystals also demonstrates an evident but nevertheless compelling fact: the explicit knowledge of the relaxation of a problem results in an enormous reduction of computational cost, and a correspondingly vast improvement in performance, with respect to methods that construct subgrid microstructures numerically "on the fly" (see, e.g., [4]). This strongly suggests that explicit relaxation results such as those collected in section 4 will inevitably play a decisive role in rendering multiscale computing feasible.

We close by pointing out some of the limitations of the framework presented in this paper. Strict separation of scales is an idealization which is never completely realized in nature. In actual materials, the process of microstructural refinement described by a minimizing sequence is checked by physical phenomena unaccounted for in the original model. For instance, in single crystals the interfaces between the variants of a laminate are dislocation walls that carry a well-defined energy per unit area [53]. Consideration of this additional energy has the effect of introducing an intrinsic length scale commensurate with the Burgers vector and is responsible for scaling laws such as the Hall–Petch effect [54, 22]. The dislocation wall energy has the additional effect of radically changing the geometry of the optimal microstructures, which tend to exhibit self-similar refinement towards the boundary [22]. Under these

conditions, the relaxed energy of, e.g., a grain is no longer local, i.e., described by an effective energy density depending solely on the deformation gradient. To the best of our knowledge, the formulation of multiscale numerical methods capable of dealing with nonlocal effective energies remains at present an open question.

REFERENCES

[1] L. Ambrosio, A. Coscia, and G. Dal Maso, *Fine properties of functions with bounded deformation*, Arch. Rational Mech. Anal., 139 (1997), pp. 201–238.

[2] G. Anzellotti and M. Giaquinta, *Existence of the displacements field for an elasto-plastic body subject to Hencky's law and von Mises yield condition*, Manuscripta Math., 32 (1980), pp. 101–136.

[3] D. N. Arnold, F. Brezzi, and M. Fortin, *A stable finite element for the Stokes equations*, Calcolo, 21 (1984), pp. 337–344.

[4] S. Aubry and M. Ortiz, *The mechanics of deformation-induced subgrain-dislocation structures in metallic crystals at large strains*, R. Soc. Lond. Proc. Ser. A Math. Phys. Eng. Sci., 459 (2003), pp. 3131–3158.

[5] J. Ball and R. D. James, *Fine phase mixtures as minimizers of the energy*, Arch. Rational Mech. Anal., 100 (1987), pp. 13–52.

[6] F. Ben Belgacem, *The mixed mortar finite element method for the incompressible Stokes problem: Convergence analysis*, SIAM J. Numer. Anal., 37 (2000), pp. 1085–1100.

[7] T. Belytschko, J. Fish, and B. E. Engelmann, *A finite element with embedded localization zones*, Comput. Methods Appl. Mech. Engrg., 70 (1988), pp. 59–89.

[8] K. Bhattacharya and G. Dolzmann, *Relaxed constitutive relations for phase transforming materials*, J. Mech. Phys. Solids, 48 (2000), pp. 1493–1517.

[9] A. Braides, Γ-*Convergence for Beginners*, Oxford University Press, Oxford, UK, 2002.

[10] F. Brezzi, L. P. Franca, and A. Russo, *Further considerations on residual-free bubbles for advective-diffusive equations*, Comput. Methods Appl. Mech. Engrg., 166 (1998), pp. 25–33.

[11] F. Brezzi, T. J. R. Hughes, L. D. Marini, A. Russo, and E. Süli, *A priori analysis of residual-free bubbles for advection-diffusion problems*, SIAM J. Numer. Anal., 36 (1999), pp. 1933–1948.

[12] C. Carstensen, K. Hackl, and A. Mielke, *Nonconvex potentials and microstructures in finite-strain plasticity*, R. Soc. Lond. Proc. Ser. A Math. Phys. Eng. Sci., 458 (2002), pp. 299–317.

[13] C. Carstensen and P. Plecháč, *Numerical solution of the scalar double-well problem allowing microstructure*, Math. Comp., 66 (1997), pp. 997–1026.

[14] W. Chen and G. Ravichandran, *Dynamic compressive behavior of ceramics under lateral confinement*, J. Physique IV, 4 (1994), pp. 177–182.

[15] W. Chen and G. Ravichandran, *An experimental technique for imposing dynamic multiaxial compression with mechanical confinement*, Experiment. Mech., 36 (1996), pp. 155–158.

[16] W. Chen and G. Ravichandran, *Static and dynamic compressive behavior of aluminum nitride under moderate confinement*, J. Amer. Soc. Ceramics, 79 (1996), pp. 579–584.

[17] W. Chen and G. Ravichandran, *Failure mode transition in ceramics under dynamic multiaxial compression*, Internat. J. Fracture, 101 (2000), pp. 141–159.

[18] P.-G. Ciarlet, *Mathematical Elasticity*, North–Holland, Amsterdam, 1988.

[19] D. Cioranescu and P. Donato, *An Introduction to Homogenization*, Oxford University Press, New York, 1999.

[20] S. Conti, A. DeSimone, and G. Dolzmann, *Semi-soft elasticity and director reorientation in stretched sheets of nematic elastomers*, Phys. Rev. E (3), 66 (2002), 061710.

[21] S. Conti, A. DeSimone, and G. Dolzmann, *Soft elastic response of stretched sheets of nematic elastomers: A numerical study*, J. Mech. Phys. Solids, 50 (2002), pp. 1431–1451.

[22] S. Conti and M. Ortiz, *Dislocation microstructures and the effective behavior of single crystals*, Arch. Ration. Mech. Anal., 176 (2005), pp. 103–147.

[23] M. Crouzeix and P.-A. Raviart, *Conforming and nonconforming finite element methods for solving the stationary Stokes equations.* I, Rev. Française Automat. Informat. Recherche Opérationnelle Sér. Rouge, 7 (1973), pp. 33–75.

[24] B. Dacorogna, *Direct Methods in the Calculus of Variations*, Springer-Verlag, New York, 1989.

[25] G. Dal Maso, *Introduction to* Γ-*Convergence*, Birkhäuser Boston, Boston, MA, 1993.

[26] A. DeSimone and G. Dolzmann, *Macroscopic response of nematic elastomers via relaxation*

of a class of $SO(3)$-invariant energies, Arch. Ration. Mech. Anal., 161 (2002), pp. 181–204.
[27] G. Dolzmann, *Numerical computation of rank-one convex envelopes*, SIAM J. Numer. Anal., 36 (1999), pp. 1621–1635.
[28] G. Dolzmann and N. J. Walkington, *Estimates for numerical approximations of rank one convex envelopes*, Numer. Math., 85 (2000), pp. 647–663.
[29] H. Le Dret and A. Raoult, *Quasiconvex envelopes of stored energy densities that are convex with respect to the strain tensor*, in Calculus of Variations, Applications and Computations (Pont-à-Mousson, 1994), Pitman Res. Notes Math. Ser. 326, C. Bandle, J. Bemelmans, M. Chipot, J. Saint Jean Paulin, and I. Shafrir, eds., Longman Scientific and Technical, Harlow, UK, 1995, pp. 138–146.
[30] M. Fago, *Constrained Sequential Lamination: Nonconvex Optimization and Material Microstructure*, Ph.D. dissertation, California Institute of Technology, Pasadena, CA, 2004.
[31] I. Fonseca, *The lower quasiconvex envelope of the stored energy function for an elastic crystal*, J. Math. Pures Appl. (9), 67 (1988), pp. 175–195.
[32] L. P. Franca, C. Farhat, A. P. Macedo, and M. Lesoinne, *Residual-free bubbles for the Helmholtz equation*, Internat. J. Numer. Methods Engrg., 40 (1997), pp. 4003–4009.
[33] L. P. Franca and A. P. Macedo, *A two-level finite element method and its application to the Helmholtz equation*, Internat. J. Numer. Methods Engrg., 43 (1998), pp. 23–32.
[34] E. De Giorgi, *Sulla convergenza di alcune sucessioni di integrali del tipo dell'area*, Rend. Mat. (6), 8 (1975), pp. 277–294.
[35] E. De Giorgi and T. Franzoni, *Su un tipo di convergenza variazionale*, Atti. Accad. Naz. Lincei Rend. Cl. Sci. Fis. Mat. Natur. (8), 58 (1975), pp. 842–850.
[36] P. Hauret, *Méthodes numériques pour la dynamique des structures non-linéaires incompressibles à deux échelles (Numerical Methods for the Dynamic Analysis of Two-Scale Incompressible Nonlinear Structures)*, Ph.D. thesis, École Polytechnique, Palaiseau Cedex, France, 2004.
[37] T. J. R. Hughes, *Multiscale phenomena: Green's function, the Dirichlet-to-Neumann formulation, subgrid scale models, bubbles and the origins of stabilized methods*, Comput. Methods Appl. Mech. Engrg., 127 (1995), pp. 387–401.
[38] T. J. R. Hughes, G. R Feijóo, L. Mazzei, and J. B. Quincy, *The variational multiscale method—a paradigm for computational mechanics*, Comput. Methods Appl. Mech. Engrg., 166 (1998), pp. 3–24.
[39] R. V. Kohn and G. Strang, *Explicit relaxation of a variational problem in optimal design*, Bull. Amer. Math. Soc. (N.S.), 9 (1983), pp. 211–214.
[40] R. V. Kohn and G. Strang, *Optimal design and relaxation of variational problems.* I., Comm. Pure Appl. Math., 39 (1986), pp. 113–137.
[41] R. V. Kohn and G. Strang, *Optimal design and relaxation of variational problems.* II., Comm. Pure Appl. Math., 39 (1986), pp. 139–182.
[42] R. V. Kohn and G. Strang, *Optimal design and relaxation of variational problems.* III., Comm. Pure Appl. Math., 39 (1986), pp. 353–377.
[43] Y. Leroy and M. Ortiz, *Finite element analysis of strain localization in frictional materials*, Internat. J. Numer. Anal. Methods Geomech., 13 (1989), pp. 53–74.
[44] Y. Leroy and M. Ortiz, *Finite element analysis of transient strain localization phenomena in frictional materials*, Internat. J. Numer. Anal. Methods Geomech., 14 (1990), pp. 93–124.
[45] Y. Leroy, M. Ortiz, and A. Needleman, *An overview of finite element methods for the analysis of strain localization*, in Cracking and Damage: Strain Localization and Size Effect, J. Mazars and Z. P. Bazant, eds., Elsevier Applied Science, New York, 1989, pp. 269–294.
[46] C. Miehe, M. Lambrecht, and E. Gürses, *Analysis of material instabilities in inelastic solids by incremental energy minimization and relaxation methods: Evolving deformation microstructures in finite plasticity*, J. Mech. Phys. Solids, 52 (2004), pp. 2725–2769.
[47] C. B. Morrey, *Quasiconvexity and the semicontinuity of multiple integrals*, Pacific J. Math., 2 (1952), pp. 25–53.
[48] C. B. Morrey, *Multiple Integrals in the Calculus of Variations*, Springer-Verlag, New York, 1966.
[49] S. Müller, *Variational models for microstructure and phase transitions*, in Calculus of Variations and Geometric Evolution Problems, Lecture Notes in Math. 1713, F. Bethuel, G. Huisken, A. Polden, S. Müller, and K. Steffen, eds., Springer-Verlag, Berlin, 1999, pp. 85–210.
[50] A. Nacar, A. Needleman, and M. Ortiz, *A finite element method for analyzing localization in rate-dependent solids at finite strains*, Comput. Methods Appl. Mech. Engrg., 73 (1989), pp. 235–258.

[51] M. Ortiz, *A variational formulation for convection-diffusion problems*, Internat. J. Engrg. Sci., 23 (1985), pp. 717–731.
[52] M. Ortiz, Y. Leroy, and A. Needleman, *A finite element method for localized failure analysis*, Comput. Methods Appl. Mech. Engrg., 61 (1987), pp. 189–214.
[53] M. Ortiz and E. A. Repetto, *Nonconvex energy minimization and dislocation structures in ductile single crystals*, J. Mech. Phys. Solids, 47 (1999), pp. 397–462.
[54] M. Ortiz, E. Repetto, and L. Stainier, *A theory of subgrain dislocation structures*, J. Mech. Phys. Solids, 48 (2000), pp. 2077–2114.
[55] A. Pandolfi, S. Conti, and M. Ortiz, *A recursive-faulting model of distributed damage in confined brittle materials*, J. Mech. Phys. Solids, 54 (2006), pp. 1972–2003.
[56] A. A. Pipkin, *Relaxed energy densities for large defomations of membranes*, IMA J. Appl. Math., 52 (1994), pp. 297–308.
[57] W. Rudin, *Functional Analysis*, McGraw–Hill, New York, 1973.
[58] Y. C. Shu and K. Bhattacharya, *Domain patterns and macroscopic behaviour of ferroelectric materials*, Philos. Mag. B, 81 (2001), pp. 2021–2054.
[59] P. Suquet, *Existence et régularité des solutions des équations de la plasticité*, C. R. Acad. Sci. Paris Sér. A-B, 286 (1978), pp. 1201–1204.
[60] R. Temam, *Mathematical Problems in Plasticity*, Bordas, Paris, 1985.
[61] V. Šverák, *Rank-one convexity does not imply quasiconvexity*, Proc. Roy. Soc. Edinburgh Sect. A, 120 (1992), pp. 185–189.